Monthly Notices
of the
ROYAL ASTRONOMICAL SOCIETY

MNRAS **428,** 205–211 (2013) doi:10.1093/mnras/sts024

Light curves of six bright soft X-ray transients in M31

Nakisa Nooraee[1,2]★

[1]*Dublin Institute for Advanced Studies, 31 Fitzwilliam Place, Dublin 2, Ireland*
[2]*University College Cork, Cork, Ireland*

Accepted 2012 September 17. Received 2012 September 11; in original form 2012 August 2

ABSTRACT

Disc irradiation is thought to be capable of explaining the global behaviour of the light curves of soft X-ray transients (SXTs). Depending on the strength of the central X-ray emission in irradiating the disc, the light curve may exhibit an exponential or a linear decay. The model predicts that in brighter transients a transition from exponential decline to a linear one may be detectable. In this study, having excluded super-soft sources and hard X-ray transients, a sample of bright SXTs in M31 ($L_{\rm peak} > 10^{38}$ erg s^{-1}) has been studied. The expected change in the shape of the decay function is only observed in two of the light curves from the six light curves in the sample. Also, a systematic correlation between the shape of the light curve and the X-ray luminosity has not been seen.

Key words: binaries: close – X-rays: binaries – X-rays: stars.

1 INTRODUCTION

Soft X-ray transients (SXTs) are a subgroup of low-mass X-ray binaries (LMXBs) consisting of a neutron star or a black hole (BH) and a companion low-mass star ($M < 1\,{\rm M}_{\odot}$). SXTs exhibit a sudden outburst by increasing the luminosity from $\sim 10^{33}$ to $\sim 10^{36-38}$ erg s^{-1}. After spending a few months in outburst, SXTs switch back to quiescence. Optical study of the binary system during the quiescence state of SXTs provides an opportunity to discriminate between BH binaries and neutron star binaries.

Optical follow-up of Galactic BH binary systems show that many stellar mass black hole systems are transient (Remillard & McClintock 2006).

The availability of high-resolution X-ray telescopes over the last decade has made it possible to look for SXTs hosted by other galaxies. One of the most regularly targeted galaxies is M31, the nearest spiral galaxy to us. Up to now, more than 50 SXTs have been detected in M31 (Kong et al. 2002; Williams et al. 2004).

Early attempts to explain the behaviour of SXTs originated from studies of dwarf novae (DNe). The principal difference between DNe and SXTs is in the compact object; DNe have white dwarfs as their compact objects. These two groups have similar behaviour, except time-scales: the outbursts of SXTs last a few months and they recur in time-scales of years where as the time-scales of DNe are days and months.

The similarities between SXTs and DNe suggested expanding the accepted model of DNe (disc instability model) to SXTs. van Paradijs (1996) showed that the disc instability model is applicable for SXTs provided that the irradiation disc effect is taken into account. Irradiation by the central X-ray emission prevents the quick cooling down and therefore elongates the outburst duration. Carrying out a test on the model by gathering a sample of the persistent and transient X-ray binaries (XRBs), it was shown that the proposed model is able to discriminate between persistent and transient X-ray emission from binary systems (van Paradijs 1996). A recent test has proven the same result (Coriat, Fender & Dubus 2012). Despite the success of the irradiated disc model in producing the global behaviour of XRBs, some features in the light curve of SXTs, e.g. glitches, plateaux and re-brightening, remain unexplained (Truss et al. 2002).

Assuming the irradiated accretion disc model for SXTs, King & Ritter (1998, hereafter KR98) concluded that depending on the strength of central X-ray, the light curve of transient may have exponential or linear decay. Linear decline is expected to happen in binary systems with longer orbital period, due to having larger accretion discs and the irradiation cannot fully ionize the disc. KR98 predicted that the light curve of brighter transients might show a transition from an exponential decay to a linear one during the outburst.

To examine the prediction of a change from an exponential decay to a linear one in the light curve of a bright transient, I acquired archival X-ray data from very bright SXTs in M31 whose peak luminosity satisfies

$$L_{\rm peak} \geq 10^{38}\ {\rm erg\ s^{-1}}.$$

In order to have the maximum possible light curves, data from three X-ray telescopes, i.e. *Chandra*, *XMM–Newton* and *Swift*/XRT are used.

The outline of the paper is as follows: Section 2 gives the details of source selection criteria and the final list of sources in this study. The analysis of sources and the light curves are individually given

★ E-mail: nakisa.nooraee@gmail.com

in Section 3. The results which are presented in Section 4 will be discussed in Section 5.

2 SOURCE SELECTION

Publicly available X-ray data of the bright sources taken with *Chandra* (ACIS), *XMM–Newton* (PN) and *Swift* (XRT) have been retrieved from the HEASARC website.[1] To have a sample only consisting of SXTs, the bright sources which satisfy the luminosity criteria but belong to other group of transients are excluded from the study as described below.

Hard X-ray transients are expected to be observed in high-mass XRBs, where the accretion disc is fed by stellar winds. This group of transient sources, even the very bright ones, are not included in this study, e.g. a very bright hard transient, CXO J004242.0+411608 (Garcia et al. 2000; Trudolyubov, Borozdin & Priedhorsky 2001) with luminosity $(1.4 \pm 0.08) \times 10^{38}$ erg s^{-1} is a hard X-ray transient and therefore removed from the study list.

A big subgroup of transient sources are super-soft X-ray sources (SSSs). It is believed that SSSs occur when matter accretes from the companion on to white dwarf, after filling the Roche lobe. SSSs exhibit bright point sources in the X-ray sky with the luminosity 10^{37}–10^{39} erg s^{-1}, even though their spectral energy of emission is not larger than 1.5 keV. For instance, XMMU J004319.4+411759 (designated name r3-126; Williams et al. 2006) exhibits luminosity $\sim 1.3 \times 10^{38}$ erg s^{-1} in 0.3–1.5 keV (Trudolyubov et al. 2001) (for more information, see Di Stefano et al. 2004).

Due to the lack of spectral information for the *Chandra* HRC camera, in order to be able to estimate the flux of the source, the count rate of the source must be converted into flux by assuming a model. To this aim, the model fitted to the spectra of the next or prior observation of the HRC one (HRC-I) is usually assumed to be valid during the HRC observation. Thus, an HRC observation is not suitable for a spectral study. In this study, no HRC observation has been used. Also, sources which have only been detected by HRC-I have been excluded e.g. due to be located far from the galaxy bulge, SWIFT J004159.3+410539 with $L_{\rm peak} \sim 4 \times 10^{38}$ erg s^{-1} (Haberl et al. 2009; Pietsch, Henze & Haberl 2009) only two detection with provide spectral information is available [*Swift* observation (ObsId 00031518002) and *Chandra*/ACIS (ObsId 10718)]. Even though the source has been observed with HRC, it is not included in this paper.

The final list of the bright sources is given in Table 1.

3 DATA ANALYSIS

The *Chandra*/ACIS data have been reduced using the `chandra_repro` task in CIAO 4.4 and CALDB 4.4.7. Spectra are extracted with `specextract` by binning data to 20 counts per bin for the sources with more than 150 counts.

SAS 11.0.0 has been used to reduce *XMM–Newton*/PN data and spectra are extracted with `evselect` along with `rmfgen` and `arfgen` to produce the response files, response matrix file (RMF) and ancillary response file (ARF), respectively.

Data reduction on *Swift*/XRT data was performed by HEASOFT 6.11. To use the latest CALDB *Swift* files, all data were reprocessed with `xrtpipeline v0.12.6` along with producing exposure maps. Using `XSELECT 2.4b`, spectra of the sources and backgrounds were extracted from a circle with the recommended radius by the *Swift* team, 20 pixel (=47 arcsec, 1 XRT pixel = 2.36 arcsec) for the source and 30 pixel (=70 arcsec) for the background. The appropriate RMF for each source is selected from the calibration data base and the ARFs were generated with `xrtmkarf`.

Using `grppha` (included in HEASOFT), *XMM*/PN and *Swift*/XRT data are binned to 20 counts per bin, in order to use the χ^2 statistic. For sources with less counts, the bin factor is reduced to 10 per bin and in the cases of very low count number, i.e. $\leq$50, data are binned to 1 count per bin and the Cash statistic is used.

During the observation of very bright sources, pileup can affect the spectra taken in a CCD camera. The pileup effect on ACIS data is examined by generating a pileup map using the `pileup_map`[2] task in CIAO. In the generated pileup map, any pixel value which is more than 0.2 count per frame indicates pileup. The pileup effect on *XMM–Newton* data for a point source with count rate above 0.7 count s^{-1} has to be checked using `epatplot`. Following the advice of the *Swift* team, sources with count rates of $\sim$0.5 count s^{-1} or above should be controlled for pileup.[3] The point spread function (PSF) of point sources in XRT is modelled using a king function $\mathrm{PSF}(r) = [1 + (r/r_c)^2]^{-\beta}$ where $r_c \sim 5.8$ and $\beta \sim 1.55$ (Moretti et al. 2006).

In order to correct the spectra of piled-up sources in ACIS observations, the implemented model `pileup`[4] in XSPEC from Davis (2001) is used. In *XMM*/PN and *Swift*/XRT observation data, central pixels are excluded by extracting the spectrum from an annulus.

Models are fitted to the spectra using XSPEC 12.7.0. The simplest version of the multicolour disc model, `diskbb` (Mitsuda et al. 1984; Makishima et al. 1986), has been employed to fit data with standard accretion disc model. Power-law model and hydrogen column density absorption are implemented as `po` and `phabs`, respectively. Using `cflux`,[5] unabsorbed fluxes are calculated in the energy range of 0.2–10.0 keV. Assuming that the distance to M31 is 780 kpc (Holland 1998), unabsorbed fluxes were converted to luminosity.

To constrain an upper limit of counts of the source before and after the outburst in ACIS observations, `aprates`[6] is used. Similarly, `eregionanalyse` constrains the upper limit in PN observations. To do the same on XRT images, `uplimit` available in XIMAGE is used. Using PIMMS and assuming a power-law model, the count rates are converted into flux and then luminosity.

Table 1. List of the bright sources.

Coordinate	Name	Outburst (d)[a]
00:42:16.1 +41:19:26.7	XMMU J004215.8+411924	32–71[b]
		22–110[c]
00:42:17.3 +41:15:37.2	SWIFT J004217.4+411532	137–180
00:42:53.2 +41:14:22.6	CXOM31 J004253.1+411422	184–259
00:43:05.6 +41:17:03.3	CXOM31 J004305.7+411703	132–222
00:43:20.56 +41:15:28.8	SWIFT J004320.5+411528	61–132

[a]The minimum duration of any outburst is determined by the interval between the first and the last X-ray detections. The upper limit is, then, given by the time interval between the previous and next observations from the first and last detections.
[b]First outburst in 2006.
[c]Re-outburst in 2010.

[1] http://heasarc.gsfc.nasa.gov/docs/archive.html

[2] http://cxc.harvard.edu/ciao/ahelp/acis_pileup.html
[3] http://www.swift.ac.uk/analysis/xrt/pileup.php
[4] http://heasarc.gsfc.nasa.gov/xanadu/xspec/manual/XSmodelPileup.html
[5] http://heasarc.nasa.gov/xanadu/xspec/manual/XSmodelCflux.html
[6] http://cxc.harvard.edu/ciao/threads/upperlimit/

3.1 Spectral analysis

Spectral analysis of the sources listed in Table 1 are presented individually here. The best-fitting parameters are summarized in Table 2. For each source, the value of hydrogen column density is determined from the best-fitting result which provides a value consistent with the hydrogen column density towards M31. In the rest of observations, $N_{\rm H}$ is frozen wherever applicable.

(i) XMMU J004215.8+411924

For the spectrum of the first detection of XMMU J004215.8+411924 (Galache et al. 2006; Haberl et al. 2006), both a power-law model and a disc blackbody model gave an acceptable

Table 2. Best spectral fit results. Parameters without uncertainty are frozen.

Date (ObsId)	Inst.[a]	T^b	$N_{\rm H}$ (10^{21})	Best-fitting parameters[c]	χ^2/dof	L^d ($\times10^{37}$)
			XMMU J004215.8+411924			
2006/07/02 (0405320501)	PN	–	3.4	$\Gamma = 1.5$	–	<0.30
2006/07/31 (7139)	ACIS	0	5.3 ± 1.5	$\Gamma = 1.9 \pm 0.2$	16.2/15	18.5 ± 3.1
2006/08/09 (0405320601)	PN	9	3.4 ± 0.07	$\Gamma = 1.6 \pm 0.1$	18.9/18	12.6 ± 1.1
2006/09/01 (00030802001)	XRT	32	3.4	$\Gamma = 1.6$	21.6/27	2.63 ± 0.6
2006/09/11 (00030804001)	XRT	–	3.4	$\Gamma = 1.6$	–	<0.41
2010/03/05 (11279)	ACIS	–	4.1	$\Gamma = 1.5$	–	<0.14
2010/05/27 (11838)	ACIS	0	4.1 ± 2.2	$\Gamma = 1.5 \pm 0.2$	7.1/10	12.9 ± 1.5
2010/06/06 (00031255012)	XRT	10	4.1	$\Gamma = 1.5$	36.2/50	9.7 ± 1.3
2010/06/09 (00031255013)	XRT	13	4.1	$\Gamma = 1.5$	34.2/42	8.1 ± 1.6
2010/06/12 (00031255014)	XRT	16	4.1	$\Gamma = 1.5$	45.9/37	8.0 ± 1.7
2010/06/15 (00031255015)	XRT	19	4.1	$\Gamma = 1.5$	24.2/23	5.7 ± 1.5
2010/06/18 (00031255016)	XRT	22	4.1	$\Gamma = 1.5$	19.1/19	4.4 ± 1.3
2010/06/23 (11839)	ACIS	–	4.1	$\Gamma = 1.5$	–	<0.10
			SWIFT J004217.4+411532			
2006/08/09 (0405320601)	PN	–	6	–	–	<0.07
2006/09/01 (00030802001)	XRT	0	5.8 ± 1.9	$T_{\rm in} = 0.63 \pm 0.04$	29.7/71	28.8 ± 2.0
2006/09/11 (00030804001)	XRT	10	6	$T_{\rm in} = 0.51 \pm 0.03$	14.4/15	22.4 ± 1.3
2006/09/24 (7140)	ACIS	23	6	$T_{\rm in} = 0.55 \pm 0.03$	24.2/25	10.6 ± 0.4
2006/12/04 (7064)	ACIS	94	6	$T_{\rm in} = 0.34 \pm 0.01$	18.3/21	3.12 ± 0.1
2006/12/31 (0405320701)	PN	121	6	$T_{\rm in} = 0.31 \pm 0.01$	101.9/58	2.04 ± 0.07
2007/01/14 (8183)	ACIS	135	6	$T_{\rm in} = 0.27$	46.8/38	1.02 ± 0.16
2007/01/16 (0405320801)	PN	137	6	$T_{\rm in} = 0.27 \pm 0.01$	30.6/25	1.26 ± 0.06
2007/02/05 (0405320901)	PN	–	6	–	–	<0.03
			CXOM31 J004253.1+411422			
2009/12/08 (11276)	ACIS	–	5	$\Gamma = 1.7$	–	<0.10
2009/12/22 (00031518013)	XRT	0	5.1 ± 1.7	$T_{\rm in} = 1.17 \pm 0.06$	65.8/61	182.5 ± 7.0
2009/12/23 (00035336016)	XRT	1	5.6 ± 1.4	$T_{\rm in} = 1.09 \pm 0.05$	67.5/78	169.5 ± 5.7
2009/12/24 (00035336017)	XRT	2	5	$T_{\rm in} = 1.23 \pm 0.05$	63.4/64	172.7 ± 6.2
2009/12/25 (00035336018)	XRT	3	5.1 ± 1.4	$T_{\rm in} = 1.14 \pm 0.05$	66.6/67	163.6 ± 5.6
2009/12/26 (00035336019)	XRT	4	5	$T_{\rm in} = 1.06 \pm 0.04$	67.2/62	154.0 ± 5.2
2009/12/27 (00035336020)	XRT	5	5	$T_{\rm in} = 1.21 \pm 0.04$	90.7/114	150.5 ± 3.7
2009/12/28 (0600660201)	PN	6	5	$T_{\rm in} = 0.90 \pm 0.01$	698.6/535	140.4 ± 1.4
2010/01/01 (11277)	ACIS	10	5	$\alpha = 0.5$, $T_{\rm in} = 0.98 \pm 0.1$	12.9/12	126.9 ± 30
2010/01/07 (0600660301)	PN	16	5	$T_{\rm in} = 0.85 \pm 0.01$	628.6/476	93.3 ± 0.9
2010/01/15 (0600660401)	PN	24	5	$T_{\rm in} = 0.79 \pm 0.01$	555.5/402	72.3 ± 0.8
2010/01/25 (0600660501)	PN	34	5	$T_{\rm in} = 0.73 \pm 0.01$	318.82/307	54.7 ± 0.7
2010/01/27 (00031518014)	XRT	36	4.4 ± 1.8	$T_{\rm in} = 0.86 \pm 0.05$	22.6/33	47.4 ± 2.3
2010/02/02 (0600660601)	PN	42	5	$T_{\rm in} = 0.64 \pm 0.02$, $\Gamma = 1.86 \pm 0.09$	464.7/379	34.5 ± 1.3
2010/02/22 (00031518015)	XRT	62	5.0	$T_{\rm in} = 0.48 \pm 0.08$, $\Gamma = 1.49 \pm 0.5$	36.2/36	14.9 ± 5
2010/05/27 (11838)	ACIS	156	5	$\Gamma = 2.2 \pm 0.1$	20.5/22	7.7 ± 0.5
2010/06/06 (00031255012)	XRT	166	5	$\Gamma = 2.5 \pm 0.2$	55.0/68	7.7 ± 1.0
2010/06/09 (00031255013)	XRT	169	5	$\Gamma = 2.2 \pm 0.3$	36.0/49	4.3 ± 0.6
2010/06/12 (00031255014)	XRT	172	5	$\Gamma = 2.2 \pm 0.3$	21.6/42	4.4 ± 0.7
2010/06/15 (00031255015)	XRT	175	5	$\Gamma = 2.2$	–	3.3 ± 1.0
2010/06/18 (00031255016)	XRT	178	5	$\Gamma = 2.2$	–	5.7 ± 1.0
2010/06/23 (11839)	ACIS	183	5	$\Gamma = 2.2$	13.8/9	4.3 ± 0.4
2010/06/24 (00031255018)	XRT	184	5	$\Gamma = 2.2$	–	4.5 ± 0.9
2010/08/24 (11841)	ACIS	–	5	$\Gamma = 1.7$	–	<0.1
2001/06/10 (1583)	ACIS	–	6.7	$\Gamma = 1.7$	–	<0.23
2001/08/31 (1577)	ACIS	0	6.7	$\alpha = 0.5$, $T_{\rm in} = 0.66 \pm 0.08$	36.0/38	30.2 ± 7.0
2001/11/19 (1585)	ACIS	80	6.7 ± 5.9	$\alpha = 0.5$, $T_{\rm in} = 0.47 \pm 0.07$	39.7/37	27.5 ± 9.0
2001/12/07 (2895)	ACIS	98	6.7	$\alpha = 0.5$, $T_{\rm in} = 0.57 \pm 0.03$	33/30	15.2 ± 1.2

Table 2 – *continued*

Date (ObsId)	Inst.[a]	T^b	N_H (10^{20})	Best-fitting parameters[c]	χ^2/dof	L^d ($\times 10^{37}$)
			CXOM31 J004305.7+411703			
2002/01/06 (0112570101)	PN	130	6.7	$\Gamma = 1.8 \pm 0.1$, $T_{in} = 0.24 \pm 0.004$	316/309	3.2 ± 1.1
2002/01/08 (2897)	ACIS	132	6.7	$\Gamma = 2.57 \pm 0.19$	13.3/13	3.3 ± 0.3
2002/02/06 (2896)	ACIS	–	6.7	$\Gamma = 1.7$	–	<0.06
			SWIFT J004320.5+411528			
2008/07/18 (0560180101)	PN	–	6.8		–	<0.08
2008/08/21 (00031255001)	XRT	−7	6.8 ± 2.8	$T_{in} = 0.57 \pm 0.05$	18.1/18	18.2 ± 1.6
2008/08/28 (00031255002)	XRT	0	6.8	$T_{in} = 0.59 \pm 0.06$	13.8/10	26.2 ± 2.0
2008/09/01 (9523)	ACIS	4	6.8	$T_{in} = 0.69 \pm 0.02$	51.7/47	22.3 ± 0.7
2008/09/04 (00031255003)	XRT	7	6.7 ± 4.1	$T_{in} = 0.72 \pm 0.09$	13.9/19	24.7 ± 2.6
2008/09/06 (00031255004)	XRT	9	6.8	$T_{in} = 0.69 \pm 0.04$	15.1/17	22.8 ± 1.7
2008/09/11 (00031255005)	XRT	14	6.8	$T_{in} = 0.68 \pm 0.04$	13.6/22	24.1 ± 1.2
2008/09/25 (00031255006)	XRT	28	6.8	$T_{in} = 0.64 \pm 0.06$	9.14/11	17.7 ± 1.2
2008/10/13 (9524)	ACIS	46	6.8	$T_{in} = 0.54 \pm 0.02$	29.7/28	12.7 ± 0.5
2008/10/14 (00031255008)	XRT	47	6.8	$T_{in} = 0.50 \pm 0.05$	5.3/9	13.3 ± 1.5
2008/10/15 (0031255009)	XRT	48	6.8	$T_{in} = 0.44 \pm 0.04$	11.7/9	11.8 ± 1.3
2008/10/21 (0003125010)	XRT	54	6.8	$T_{in} = 0.48 \pm 0.05$	21/20	9.7 ± 1.0
2008/11/27 (9521)	ACIS	–	6.8	$\Gamma = 1.7$	–	<0.22

[a] X-ray detector.
[b] Time according to *X*-axis in the light curves shown Fig. 1.
[c] Best-fitting parameters from XSPEC. Γ and T_{in} (in KeV) are for power index from a power-law model and the temperature at the inner disc radius in the `diskbb` model, respectively. α is the grade morphing parameter in `pileup` model.
[d] Unabsorbed luminosity in energy band 0.2–10.0 keV. Assumed distance is 780 kpc.

fit, but the obtained value for T_{in} is higher than the expected temperature for an accretion disc, so the data were fitted with a power-law model.

Due to the small count number in the last observation (ObsId 00030802001), the parameters are frozen to the values of previous observation fit along using the Cash statistic.

The second outburst of the source is detected 4 yr later (Noorraee et al. 2010; Barnard et al. 2011) in an ACIS observation (ObsId 11838). Fitting a power-law model gives a better fit when compared to a disc blackbody model. The following XRT observation data did not have enough count number, so using the Cash statistic, the parameters are frozen to the best-fitting parameters for the ACIS data.

Barnard et al. (2011) noted that the position of the source (on the second outburst) is just 1.6 arcsec from the position of source number 17 (Crampton et al. 1984) listed from the *Einstein* HRI observation and have concluded that this source had a detected outburst over 30 yr ago. Optical studies during the 2006 outburst (Voss et al. 2008) and 2010 outburst (Barnard et al. 2011) could not rule out a Be companion star; therefore, the host binary system of this X-ray transient is most likely to be an LMXB. So this was categorized as an SXT in the present study.

The X-ray light curves of the first outburst and re-outburst are shown in Figs 1(a) and (b), respectively.

(ii) SWIFT J004217.4+411532

Detected first by a *Swift* observation in 2006 September (Haberl et al. 2006; Voss et al. 2008), SWIFT J004217.4+411532 during ∼140 d outburst appeared in seven X-ray observations. A disc blackbody model, in all of seven observations, gives the best-fitting result. The photon numbers in ObsId 8183 are not enough to carry out a fit. Thus, data are binned to 1 count per bin and fitted parameters are frozen to the values of the *XMM* observation taken 2 d earlier. The light curve is plotted in Fig. 1(c).

(iii) CXOM31 J004253.1+411422

This very bright source detected in 2009 December with a *Chandra*/HRC observation (Henze et al. 2009) and its outburst lasted for about 200 d (Kaur et al. 2012; Middleton et al. 2012; Nooraee et al. 2012).

Due to the lack of spectral information in HRC observations and being excluded from this study, the *Swift*/XRT observation which is taken 5 d after the HRC detection has been assumed as the first point in the light curve. The extreme brightness of the source caused a pileup effect on the most of the exposures in the first two months, as explained below.

The first five *Swift* observations (ObsIds 00031518013, 00035336016, 00035336017, 00035336018 and 00035336019) with the count rate of >0.5 count s^{-1} are affected by pileup. After removing the central part of the point source, a disc blackbody model has been fitted to the spectrum. The next observation (ObsId 00035336020), with count rate 0.50 ± 0.01 count s^{-1}, does not show any pileup.

The next observation of the source was taken by *Chandra*/ACIS-I on 2009 December 27 (ObsId 10719). The *Chandra* observations of this source were taken using *alternating exposure mode* which generates two images. The severity of the pileup on the spectrum was so strong that even the shorter exposure image could not be used to fit a model to data and has been excluded from the sample (table 1 in Nooraee et al. 2012). Fitting a disc blackbody model to the next ACIS observation ObsId 11277 gives a reasonable fit. This spectra of the source show pileup, and the image with shorter exposure has been used.

Next, *XMM* observations (ObsIds 0600660201, 0600660301, 0600660401 and 0600660501) showed pileup effect which could be fitted by a disc blackbody model using spectrum from an annulus.

The source spectrum of the *Swift*/XRT observation (ObsId 00031518014) is not piled up and a disc blackbody fits the data reasonably. Due to the pile effect, the spectrum in ObsId 0600660601 was extracted from an annulus. Fitting a disc blackbody and a

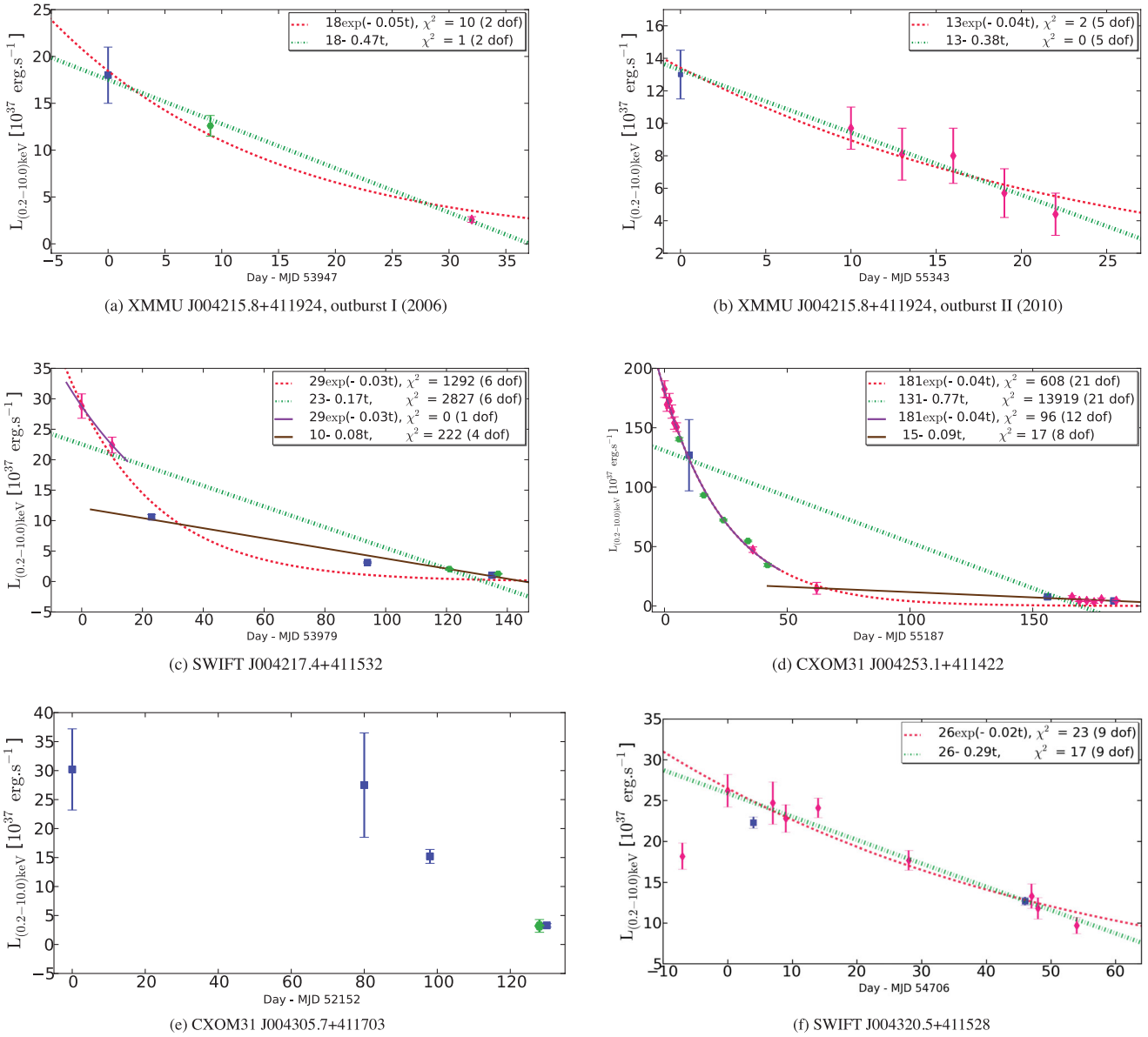

(a) XMMU J004215.8+411924, outburst I (2006)

(b) XMMU J004215.8+411924, outburst II (2010)

(c) SWIFT J004217.4+411532

(d) CXOM31 J004253.1+411422

(e) CXOM31 J004305.7+411703

(f) SWIFT J004320.5+411528

Figure 1. X-ray unabsorbed light curve of the sources. Details of best-fitting parameters are given in Table 2. Plot symbols: the blue square is *Chandra*/ACIS, the green hexagonal is *XMM*/EPIC-PN and the red diamond is *Swift*/XRT.

power-law model to data gives a better fit. The result of this fit and a disc blackbody only is compared with *Ftest*.[7] The small value of Ftest shows that the composition of a power-law model and a disc blackbody model is the correct model. Carrying out Ftest on the next XRT observation (ObsId 00031518015) shows that the composition of a disc blackbody model and a power-law model is a better fit than a power-law model. Between these two XRT observations, the source was observed once with ACIS (ObsId 11278). The severity of pileup indicates that the image with shorter exposure must be used. The spectra of the before and after observations are fitted with a disc blackbody and a power-law model; therefore, this data point has to be fitted with the same models along with a pileup model. The severity of pileup effect and the low number of counts did not allow a reasonable fit, and the fit results were not physical. So, this point is ignored in the light curve.

[7] https://heasarc.gsfc.nasa.gov/xanadu/xspec/manual/XSftest.html

A power-law model gives an acceptable fit to the rest of the spectra. The spectrum of three XRT observations (ObsId 00031255012, 00031255013 and 00031255016) was binned to 1 count per bin and the Cash statistic was employed. The count number in the next two XRT observations (ObsIds 00031255015 and 00031255016) was not enough, so the count rate was calculated from `SOSTA` (available in XIMAGE) and converted to flux using PIMMS. The same method, also, is used for the last *Swift* observation (ObsId 00031255018). The count in ACIS observation (ObsId 11839) is binned to 10 count per bin. The light curve is shown in Fig. 1(d).

(iv) CXOM31 J004305.7+411703

Discovered first in a *Chandra*/ACIS-I observation in 2001 August (Kong et al. 2001), the source has been observed in six X-ray observations throughout the outburst which lasted for approximately 140 d.

In the first four *Chandra*/ACIS observations (ObsIds 1577, 1575, 1585 and 2895) the source spectrum is piled up. A pileup model and

a disc blackbody were fitted to all the spectra except ObsId 1575. The severity of pileup in the spectrum of the source in ObsId 1575, which was taken 35 d after the first discovery, could not be fixed by fitting a pileup model and the fit result was unacceptable, so this observation has been removed from the study. Obtained values from fitting a pileup and a disc blackbody model to the other three ACIS observations were acceptable.

Fitting a disc blackbody and a power-law model to the next observation (ObsId 0112570101) gives a very good fit result, whereas a disc blackbody could not fit the data.

To the last observation (ObsId 2897), a power-law model fits the data perfectly. The light curve of the source is shown in Fig. 1(e).

(v) SWIFT J004320.5+411528

Seven days after the first detection as a new transient in a *Swift*/XRT observation (Pietsch et al. 2008), SWIFT J004320.5+411528 showed an increase in the luminosity from 1.82×10^{38} to 2.62×10^{38} erg s^{-1}. Fitting a disc blackbody model to the spectrum for both observations gives an acceptable result. Therefore, the first detection can be recognized as a pre-outburst point in the X-ray light curve.

The photons in three XRT observations (ObsIds 00031255003, 00031255008 and 00031255010) were binned to 10 count per bin. Due to the short exposure time (2 ks) in ObsId 00031255009, data were binned to 1 count per bin and the Cash statistic was used. Fitting a disc blackbody model to all of the spectrum, throughout the outburst, gives the best-fitting result. The light curve of SWIFT J004320.5+411528 is shown in Fig. 1(f).

4 RESULTS

The X-ray spectra from neutron star binary systems are composed of a blackbody component and a softer component, most probably emitted from the accretion disc. Due to absence of physical surface, the X-ray spectrum of a BH binary is assumed to consist of a soft component and a hard power-law tail. The characteristic temperature of the soft component in a neutron star binary system is ∼1.5 keV (when $L_{\rm x} \sim 10^{38}$ erg s^{-1}), while a lower temperature ($\leq$1.2 keV) has been observed from the BH binary systems (Tanaka & Shibazaki 1996). The values of $T_{\rm in}$ in Table 1 suggest that the SXTs in the study are BH binary systems, even though it should noted that the X-ray spectrum of a binary system alone cannot provide evidence for the presence or absence of a BH in the system.

Carrying out a statistical study of the X-ray light curves of Galactic SXTs, Chen, Shrader & Livio (1997) classified the light curves into five morphological types: fast-rise exponential-decay (FRED), triangular, plateau, variable decay and multipeak. Their study showed that FRED was the most frequent morphology. In this study, except CXOM31 J004305.7+411703 which shows a plateau shape, the morphology of the rest of the light curves is consistent with the result of Chen et al. (1997). Due to the plateau-shaped light curve, the light curve of CXOM31 J004305.7+411703 (Fig. 1e) can neither be fitted to an exponential nor linear function.

A linear function fits better than an exponential one to the three light curves in this sample: both outbursts of XMMU J004215.8+411924 (Figs 1a and b) and SWIFT J004320.5+411528 (Fig. 1f). To fit a function to the light curve of SWIFT J004320.5+411528, the first data point which is not the maximum luminosity is assumed as pre-outburst point and excluded from the fit.

The best fit for the two X-ray light curves in this sample, SWIFT J004217.4+411532 (Fig. 1c) and CXOM31 J004253.1+411422 (Fig. 1d), is an exponential fit followed by a linear function. Data points in the light curve of CXOM31 J004253.1+411422 are divided into two groups. Data in the first group are fitted by a disc blackbody and a disc blackbody plus a power law, while the spectra of the data points in the second group are all fitted with a power-law model. The same discrimination cannot be claimed for the light curve of SWIFT J004217.4+411532, since all of its data points are fitted by a disc blackbody model.

5 DISCUSSION

In the KR98 model, the decay constant in the exponential decay represents the viscous time of the outer accretion disc. Comparing the decay constant time of the exponential fit to the light curves in Fig. 1 (20, 25, 33, 25 and 50 d) with the Galactic SXTs with exponential decays, i.e. A0620−00 ($\tau \sim 24$ d), J0422+32 ($\tau \sim 40$ d) and 2000+251 ($\tau \sim 30$ d) (Tanaka & Shibazaki 1996), shows consistency.

In the disc irradiation model, the amount of irradiation is an important parameter. If the central X-ray source is strong enough to irradiate the disc entirely, then the size of the irradiated disc can be estimated from Kepler's law and Roche geometry. Therefore, one can derive scaling laws between the orbital period and the evolutionary state of the binary system. Binary systems with longer orbital periods are assumed to have longer outburst decay constants. However, KR98 predicted that the decay constants of the binary systems with orbital periods of longer than a day saturate at ∼40 d. They also noted that for longer orbital period systems (therefore bigger accretion discs) one should expect a linear decline [e.g. GRO J1744−28, the binary system with the longest orbital period among Galactic SXTs (12 d) showed a light curve with an entire linear decline]. Unfortunately, due to the large distance, optical follow-up of SXTs in M31 is not possible. However, using optical observations with the *Hubble Space Telescope* and the empirical relationship between X-ray luminosity and optical magnitude, Barnard et al. (2012) constrained the orbital period for 12 SXTs in M31 which includes estimates for the orbital period of three binary systems in this paper [here the orbital period estimated by the M12 method in table 2 of Barnard et al. (2012) is used]. The estimated orbital periods for the SXTs of M31 in this study ($P = 11.6$ h for XMMU J004215.8+411924, 16^{+7}_{-5} h for SWIFT J004217.4+411532 and 18^{+5}_{-6} h for CXOM31 J004253.1+411422) are not longer than a day. Thus, it is not possible to compare these systems with the above KR98 predictions or the Galactic SXTs.

The light curves of the six bright sources in this study suggest that the X-ray luminosity may not be the only determining factor for the shape of decline function of the light curve. Even though all the sources in this study can be classified in the group of brighter sources in M31, just two out of six light curves show an exponential followed by a linear fit.

This study does not indicate any systematic correlation between the spectral evolution and the shape of light curve, e.g. despite having similar light-curve shape, SWIFT J004217.4+411532 (Fig. 1c) does not show any spectral change throughout its outburst while CXOM31 J004253.1+411422 (Fig. 1d) clearly shows two different spectral changes. Also, the spectral model of the data points cannot predict the shape of light curve, e.g. all data points of SWIFT J004217.4+411532 and SWIFT J004320.5+411528 are fitted with the disc blackbody model; the light curve of the first one is fitted by an exponential function followed by a linear while the light curve of the later shows a linear decline is the best fit.

6 CONCLUSION

In this study, excluding hard X-ray transients and super soft sources from the sample, bright SXTs in M31 ($L_{\rm peak} > 10^{38}\,{\rm erg\,s^{-1}}$) have been used to investigate any correlation between X-ray luminosity and the decline function of the light curve. In only two of the light curves, an exponential followed by a linear function gave the best fit to the light curves. Three light curves showed that a linear decay may describe them better than an exponential.

Despite the small number of light curves in the sample, it is clear that a transition from exponential to linear decay in bright SXTs is not a global feature of the bright sources and must depend on parameters other than the X-ray luminosity of the source.

ACKNOWLEDGMENTS

This research has made use of data obtained through the High Energy Astrophysics Science Archive Research Center Online Service, provided by the NASA/Goddard Space Flight Center.

The author would like to thank Paul Callanan for providing very helpful comments on the initial draft. Also, the author wishes to thank the referee whose comments helped to improve substantially the discussion section.

REFERENCES

Barnard R., Garcia M., Murray S., Nooraee N., Pietsch W., 2011, A&A, 526, A50
Barnard R., Galache J. L., Garcia M. R., Nooraee N., Callanan P. J., Zezas A., Murray S. S., 2012, ApJ, 756, 32
Chen W., Shrader C. R., Livio M., 1997, ApJ, 491, 312
Coriat M., Fender R. P., Dubus G., 2012, MNRAS, 3347
Crampton D., Hutchings J. B., Cowley A. P., Schade D. J., van Speybroeck L. P., 1984, ApJ, 284, 663
Davis J. E., 2001, ApJ, 562, 575
Di Stefano R. et al., 2004, ApJ, 610, 247
Galache J. L., Garcia M. R., Torres M. A. P., Murray D. S. S. S., Primini F. A., Williams B. F., 2006, The Astron. Telegram, 969, 1
Garcia M. R., Murray S. S., Primini F. A., Forman W. R., McClintock J. E., Jones C., 2000, ApJ, 537, L23
Haberl F., Pietsch W., Greiner J., Ajello M., 2006, The Astron. Telegram, 881, 1
Haberl F., Henze M., Pietsch W., Orio M., 2009, The Astron. Telegram, 2262, 1
Henze M., Pietsch W., Haberl F., Greiner J., 2009, The Astron. Telegram, 2356, 1
Holland S., 1998, AJ, 115, 1916
Kaur A. et al., 2012, A&A, 538, A49
King A. R., Ritter H., 1998, MNRAS, 293, L42 (KR98)
Kong A., Garcia M., Murray S., Primini F., McClintock J., Di Stefano R., 2001, The Astron. Telegram, 76, 1
Kong A. K. H., Garcia M. R., Primini F. A., Murray S. S., Di Stefano R., McClintock J. E., 2002, ApJ, 577, 738
Makishima K., Maejima Y., Mitsuda K., Bradt H. V., Remillard R. A., Tuohy I. R., Hoshi R., Nakagawa M., 1986, ApJ, 308, 635
Middleton M. J., Sutton A. D., Roberts T. P., Jackson F. E., Done C., 2012, MNRAS, 420, 2969
Mitsuda K. et al., 1984, PASJ, 36, 741
Moretti A. et al., 2006, inHolt S. S., Gehrels N., Nousek J. A., eds, Proc. AIP Conf Ser. Vol. 836, In-flight calibration of the Swift XRT Point Spread Function. Am. Inst. Phys., New York, p. 676
Nooraee N., Callanan P. J., Barnard R., Garcia M. R., Murray S. S., Moss A., 2012, A&A, 542, A120
Noorraee N., Barnard R., Pietsch W., Callanan P., Garcia M., 2010, The Astron. Telegram, 2682, 1
Pietsch W., Burwitz V., Greiner J., Henze M., Stiele H., 2008, The Astron. Telegram, 1674, 1
Pietsch W., Henze M., Haberl F., 2009, The Astron. Telegram, 2287, 1
Remillard R. A., McClintock J. E., 2006, ARA&A, 44, 49
Tanaka Y., Shibazaki N., 1996, ARA&A, 34, 607
Trudolyubov S. P., Borozdin K. N., Priedhorsky W. C., 2001, ApJ, 563, L119
Truss M. R., Wynn G. A., Murray J. R., King A. R., 2002, MNRAS, 337, 1329
van Paradijs J., 1996, ApJ, 464, L139
Voss R., Pietsch W., Haberl F., Stiele H., Greiner J., Sala G., Hartmann D. H., Hatzidimitriou D., 2008, A&A, 489, 707
Williams B. F., Garcia M. R., Kong A. K. H., Primini F. A., King A. R., Di Stefano R., Murray S. S., 2004, ApJ, 609, 735
Williams B. F., Naik S., Garcia M. R., Callanan P. J., 2006, ApJ, 643, 356

This paper has been typeset from a TEX/LATEX file prepared by the author.